Austin Journal of Reproductive Medicine & Infertility

Open Access

Austin Publishing Group

Review Article

Dinitrosyl Iron Complexes with Glutathione Suppress Surgically Induced Experimental Endometriosis in Rats

Vanin AF[1]*, Burgova EN[1] and Adamyan LV[2]
[1]Semenov Institute of Chemical Physics, Russian Academy of Sciences, Russia
[2]Reproductive Medicine and Surgery, Moscow University of Medicine and Dentistry, Russia

***Corresponding author:** Anatolii F Vanin, Semenov Institute of Chemical Physics, Russian Academy of Sciences, Moscow, Russia

Received: July 06, 2015; **Accepted:** August 05, 2015; **Published:** August 08, 2015

Abstract

The review describes the results of our most recent investigations into miscellaneous effects of Dinitrosyl Iron Complexes (DNIC) with Glutathione and S-Nitrosoglutathione (GS-NO) as donors of Nitric Monoxide (NO) on the development of surgically induced endometriosis in rats. Whereas DNIC induced selective suppression of the growth of endometrioid tumors in implantation niduses, GS-NO enhanced tumour growth and lowered the immune responsiveness of experimental rats. It was suggested that the selective cytotoxic action of DNIC with glutathione on endometrioid tumors is a result of DNIC decomposition by endogenous iron chelators generated by tumor cells in order to provide the latter with iron required for fast tumor growth. The nitric monoxide released from DNIC either inside tumor cells or in their vicinity is oxidized to cytotoxic peroxynitrite and thus contributes to the strictly selective cytotoxic effect of DNIC on tumor cells. Such selectivity is not specific to GS-NO whose decomposition is spontaneous and can take place in different divisions of the abdominal cavity.

Keywords: Dinitrosyl iron complexes; Nitric oxide; S-Nitrosothiols; Endometriosis

Abbreviations

B-M-DNIC: Binuclear or Mononuclear Dinitrosyl Iron Complexes; EMT: Endometrioid Tumors; EPR: Electron Paramagnetic Resonance; GS-NO: S-nitrosoglutathione; MNIC-DETC: Mononitrosyl Iron Complexes with Diethyldithiocarbamate; RCRPC: Russian Cardiological Research-and-Production Complex; RS-NO: S-Nitosothiol

Introduction

Previous studies carried out by the members of our research team at the Semenov Institute of Chemical Physics of the Russian Academy of Sciences have established that exogenous water-soluble Dinitrosyl Iron Complexes (DNIC) with glutathione as Nitric Monoxide donors (NO) can selectively suppress the development of experimental endometriosis in rats induced by surgical transplantation of two 2-mm fragments of uterine tissue onto the inner surface of the abdominal wall [1-3]. This effect is manifested in early and more advanced steps of tumor growth. Another NO donor, viz., S-nitrosoglutathione, exerts a non-selective suppressive effect (if any) on tumor growth, which is directed against both endometrioid tumours and other tissues. By weakening the immune responsiveness in experimental animals, S-nitrosoglutathione drastically enhances tumor growth in some of them. This paper is an overview of the results of our studies into miscellaneous effects of DNIC with glutathione on the development of surgically induced experimental endometriosis in rats. It was established that the selectivity of cytotoxic effects of DNIC on endometrioid tumors is determined by their physico-chemical characteristics and the ability to undergo decomposition inside or in the vicinity of endometrioid tumours with a release of considerable amounts of NO.

Dinitrosyl Iron Complexes with Glutathione Represent a "Working Form" of Nitric Monoxide (NO), One of the Most Universal Regulators of Biological Processes

It has been established that Nitric Monoxide (NO), one of the simplest chemical compounds synthesized from L-arginine by the enzymatic route in the presence of three isoforms of NO-Synthesis (NOS), functions as one of the most universal regulators of an immense variety of biological processes occurring in human and animal organisms [4]. This activity is usually manifested at micro molar steady-state concentrations of NO synthesized by constitutive isoforms of NOS, viz., the endothelial (eNOS) and neuronal (n-NOS) is forms [1]. At steady-state concentrations of NO ≥100 μM generated by inducible NOS (iNOS), NO molecules, or, more specifically, the product of their interaction with the superoxide, viz., Peroxynitrite ($ONOO^-$) exerts various cytotoxic effects on cells and tissues by acting as a potent effector of cell-mediated immunity [4-6]. At physiological pH, the protonation of peroxynitrite gives a hydroxyl radical and nitrogen dioxide; both products are responsible for the cytotoxic effect of peroxynitrite [4,5]. Being free-radical compounds, NO and superoxide anions easily interact with each other by the diffusion-controlled mechanism resulting in a fast decrease of the NO content in cells and tissues. To prevent the NO decrease, the Nature utilizes the ability of NO to initiate the reversible formation in biological systems of endogenous nitroso derivatives, viz., S-Nitrosothiols (RS-NO) and Dinitrosyl Iron Complexes (DNIC) with thiol-containing ligands [7-9], which are responsible for stabilization, deposition, migration and transfer of NO to its biological targets. DNIC with thiol-containing ligands, which are easily synthesized by the chemical route, exist in both paramagnetic, EPR-active mononuclear

Citation: Vanin AF, Burgova EN and Adamyan LV. Dinitrosyl Iron Complexes with Glutathione Suppress Surgically Induced Experimental Endometriosis in Rats. Austin J Reprod Med Infertil. 2015; 2(4): 1019.

(M-DNIC) and diamagnetic, EPR-silent binuclear (B-DNIC) forms; their chemical formulas appear as $\{(RS^-)_2 Fe(NO)_2\}$ and $\{(RS^-)_2 Fe_2(NO)_4\}$, respectively [10-13]. B-DNIC represent thioethers of thiol-containing compounds (e.g, glutathione or cysteine) and Roussins's red salt (chemical formula $\{(S)_2 Fe_2(NO)_4\}$) [10]. The concentration of M- and B-DNIC with thiol-containing ligands is determined by the chemical equilibrium shown in (Scheme 1):

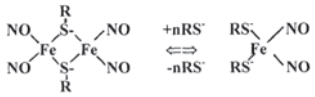

In the presence of thiol excess (or, more specifically, of thiols ionized at their sulfur atoms), the M-form dominates the solution; in the case of its deficit, it is the B-form that is predominant. It was shown [14] that M-DNIC are especially abundant in cultured animal cells; in animal tissues, DNIC with thiol-containing ligands are largely represented by the binuclear form [15]. The biological activity of DNIC with thiol-containing ligands is determined by the ability of their iron-dinitrosyl fragments to produce neutral molecules of NO and Nitrosonium Ions (NO^+) in full conformity with the chemical equilibrium between these fragments and their constituent components, viz, iron ions and nitrosyl ligands (Scheme 2) [10,16]:

$$Fe^+(NO^+)_2 \Leftrightarrow Fe^{2+} + NO + NO^+$$

The distribution of the spin density in $Fe^+(NO^+)_2$ shown in Scheme 2 is consistent with the mechanism of formation of M-DNIC with thiol-containing ligands established in our previous studies [10,16-18] (Scheme 3):

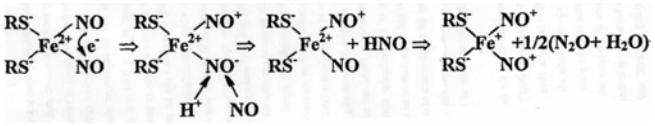

It was conjectured that binding of two NO molecules to Fe^{2+} ions in the initial steps of DNIC formation leads to their disproportionation (reciprocal single-electron oxidation-reduction), whereupon one NO molecule is converted into a nitrosonium ion (NO^+), while the other one yields a Nitroxyl Ion (NO^-). This conversion is a distinguishing feature of the NO molecule; it is manifested in the gaseous phase and at high pressures and is described by the stoichiometric reaction depicted in (Scheme 4) [19]:

$$3NO \rightarrow NO_2 + N_2O$$

The protonation of the nitroxyl ion (Scheme 3) is accompanied by its transformation into a Nitroxyl molecule (HNO), which further dissociates from the complex; subsequent recombination of two HNO molecules gives nitrous oxide (N_2O) and water. The coordination site of M-DNIC is immediately occupied by another NO molecule giving rise to paramagnetic M-DNIC with the d^7 electronic configuration of the iron atom (Fe^+). The distribution of the spin density in the $Fe(NO)_2$ fragments in the form of $Fe^+(NO^+)$ is equivalent to the formula $Fe^{2+}(NO^+)(NO)$ ($[Fe(NO)_2]^7$ in the Enemark-Feltham classification) [20]. Subsequent dimerization of M-DNIC yields B-DNIC (Scheme 1).

Judging from the distribution of the spin density in $Fe(NO)_2$ fragments, their nitrosyl ligands represent easily hydrolyzable nitrosonium ions which do not confer stability on both types of DNIC. However, in reality the situation is different, if we take into consideration the formation, in DNIC, of molecular orbital's, which include d-orbital's of iron and π-orbital's of thiol-containing and nitrosyl ligands. High π-donor activity of sulfur atoms in thiol-containing ligands enables effective transfer of shared electronic density (unshared electron pairs) from sulfur atoms to nitrosonium ions with high -acceptor activity. As a result, the values of the positive charge on these ions, which determines their interaction with hydroxyl ions and, as a consequence, the hydrolysis of nitrosonium ions, may decrease. This, in turn, hinders the hydrolysis of nitrosyl ligands in DNIC without any effect on the distribution of spin density in these DNIC [16].

If, for one reason or another, thiol-containing ligands are released from M-DNIC, e.g, after establishing of a chemical equilibrium between M-DNIC and their constituent components, the distribution of the electron density between $Fe(NO)_2$ fragments takes a pattern characteristic of electron spin density. This reaction is accompanied by a release of NO molecules and nitrosonium ions (Scheme 2). The transfer of shared electronic density from bridging sulfur atoms in B-DNIC to iron atoms and nitrosyl ligands may significantly decrease the electron density on their sulfur atoms. It is particularly this decrease that determines the remarkable ability of B-DNIC with thiol-containing ligands to retain stability in strongly acidic media. Low electron density on thiol sulfur atoms drastically reduces the risk of their protonation and thus strengthens the bonding between thiol-containing ligands and iron atoms [16,21].

The biological activity of M- and B-DNIC with thiol-containing ligands, which is determined by their ability to act as nitrosonium ion and NO donors [16,21], simulates the biological activity of endogenously produced NO. Similarly to endogenous NO, DNIC exert both beneficial (regulatory) and detrimental (cytotoxic) effect on various body cells and tissues. The former is a result of NO-induced activation of guanylate cyclase, one of the key regulatory enzymes in cell signaling system [22], which, in its turn, is due to the ability of NO molecules to bind to heme iron in guanylate cyclase. This binding is accompanied by the formation of nitrosyl complexes of heme iron and can significantly change the conformation of the protein globule and thus modulate the biological activity of heme-containing proteins. As regards nitrosonium ions released from DNIC, their biological activity is due to their ability to initiate S-nitrosation of thiol-containing proteins and interfere with their biological activity [23, 24].

As above, DNIC with natural thiol-containing ligands, e.g, glutathione or L-cysteine, can be easily prepared by chemical synthesis [10,25,26]. These DNIC are readily soluble in water, do not exert cytotoxic effects on biological objects and can be used with equal efficiency in animal studies and in experiments on isolated tissues and cell cultures. Our recent studies carried out in collaboration with researchers from other laboratories demonstrated a beneficial (regulatory) effect of exogenous water-soluble DNIC with various ligands (for the most part, with glutathione) on a vast variety of physiological processes occurring in human and animal organisms and even in plants (Table 1). The design of a novel DNIC-based hypotensive drug, which got the name Oxacom®, is one of the most impressive recent achievements in this area. After completion of pharmacological and clinical trials, which demonstrated high

Table 1: The regulatory effects of DNIC with thiol-containing ligands on various physiological processes.

1	Potent vasodilatory and hypotensive effects	[27-31]
2	Inhibition of platelet aggregation	[32-34]
3	Antihypoxic effect on the myocardium	[35]
4	Increase of red blood cell viscosoelasticity	[36]
5	Acceleration of skin wound healing	[37,38]
6	Beneficial effect on rats with hemorrhage	[39]
7	Potent penile erective activity	[40]
8	Reduction of the size of the necrotic zone in experimental myocardial infarction	[41]
9	Antiapoptotic effect on cultured normal animal and human cells	[42, 43]
10	Activation/inhibition of expression of certain genes	[44-48]
11	Enhanced assimilation of iron by plants with yellow rust disease	[49]

therapeutic activity of the new drug [31], Oxacom was put into mass production. The successful outcome of the pharmacological trials prompted the idea to examine the hypotensive activity of the drug on healthy volunteers. In a new series of our experiments, a 3-4 min single (bolus) intravenous infusion of Oxacom (3-4 ml) at a dose corresponding to 0.1 μmoles of B-DNIC with glutathione per kg of body mass caused a fast (within several minutes) drastic (by ~ 20%) drop of both systolic and diastolic pressure (from 137±4 to 110±4 mm Hg and from 85±2 to 61±4 mm Hg, respectively). During the next 6-9h, the arterial pressure remained at a sufficiently low level with a return to normal values after patient's wakening on the next day. As stated earlier in this chapter, clinical trials of Oxacom as an effective tool for relieving hypertensive crises in human patients have already been launched. Studies in this area are currently under way at the Russian Cardiological Research-and-Production Complex (RCRPC) in Moscow, at the Tomsk Cardiology Research Center and at other clinical establishments of Russia. The encouraging results of the pioneering studies [50] allowed us to recommend Oxacom as a highly effective hypotensive remedy for routine clinical practice. High clinical efficiency of Oxacom can be illustrated in the following example. A 60-year-old male patient with a diagnosed acute hypertensive crisis was admitted to the in-patient department of RCRPC. A single intravenous dose of Oxacom (0.3 μ moles of DNIC with glutathione per kg of body mass) caused a fast (within 30 min) drop of both systolic and diastolic pressure (from 240/140 mm Hg to 120/80 mm Hg), which remained at this level up to the moment of the patient's discharge from the hospital (Figure 1). The cytotoxic effect of DNIC with thiol-containing ligands is manifested under conditions of their fast decomposition with a simultaneous release of significant amounts of free NO and nitrosonium ions. A natural question arises: what mechanism is responsible for this phenomenon? The decomposition of DNIC can take place in response to acidification of intracellular compartments of DNIC or after treatment of the latter with iron chelators. As can be inferred from the aforecited data, such decomposition can hardly be related to acidification of the intracellular medium because of sufficiently high acid resistance of B-DNIC with thiol-containing ligands [21]. As regards the M-form of B-DNIC, acidification is accompanied by the conversion of B-DNIC into acid-resistant B-DNIC with a decrease in the number of thiol-containing ligands ionized at the sulfur atom (Scheme 1). Iron chelators or, more specifically, bivalent iron (Fe^{2+}) chelators destroy both forms of

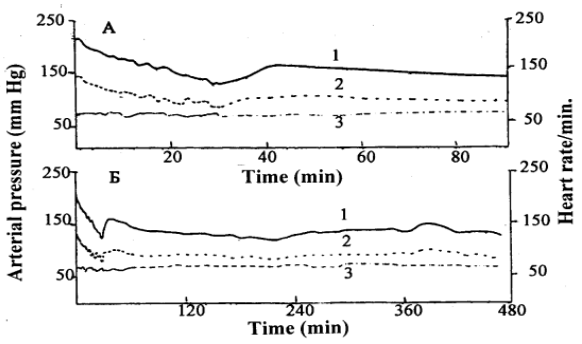

Figure 1: The dynamics of changes in the systolic (1) and diastolic (2) pressure and the pulse rate (3) of a 60-year-old male patient with hypertensive crisis (240/140 mm Hg before treatment) after a single intravenous infusion of Oxacom (7.5 mg/kg or 0.3 μmoles DNIC with glutathione/kg) 90 min (A) and 480 min (B) after treatment. (The data were kindly supplied by Academician E.I. Chazov).

DNIC with a concomitant release of nitrosyl ligands (predominantly in the form of neutral NO molecules). Supporting evidence in favor of this hypothesis was obtained in experiments where B-DNIC with glutathione underwent decomposition by *o*-phenanthroline, one of the most potent chelators of bivalent iron [21]. These data suggest that nitrosonium ions released from DNIC according to Scheme 2 were further reduced to NO by bivalent iron within the complex with *o*-phenanthroline.

Studies on cultured HeLa cells established that decomposing DNIC with glutathione or thiosulfate ligands (≤ 0.5 mM) cannot themselves produce a cytotoxic (proapoptotic) effect on HeLa cells [51]. The cytotoxic activity of these DNIC was studied cytofluorimetrically by fluorescence quenching of ethidium bromide intercolated into HeLa cell DNA. The fluorescence intensity of DNIC-Glutathione-treated HeLa cells was maintained at a level

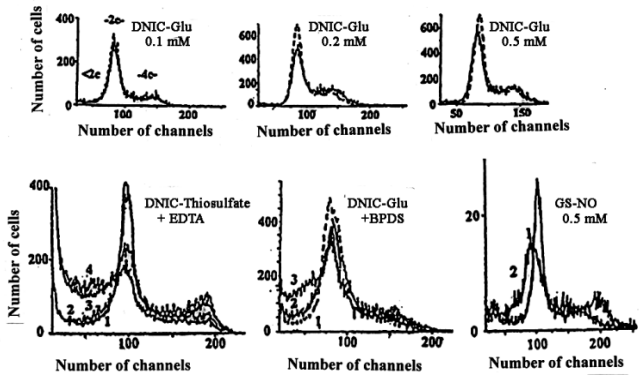

Figure 2: Upper panel: The histograms illustrating the lack of the proapoptotic effect of DNIC with glutathione (0.1, 0.2 and 0.5 mM) on HeLa cells after 22h incubation in Eagle's medium. Solid lines - control, dotted lines – experimental animals. Lower panel: The histograms illustrating the proapoptotic effects of 0.05, 0.1 and 0.2 mM DNIC with thiosulfate (curves 2-4). The cells were incubated in 0.5 mM Versene's solution (EDTA) for 22h; middle – incubation of 0.2 mM DNIC with glutathione in the presence of 0.05 mM Bathophenanthroline Disulfonate (BPDS) (curve 3); right – 0.5 M GS-NO (curve 2). The cells were incubated in Eagle's medium. In all histograms, curve 1 is control. The left and central histograms (curves 2) - incubation of HeLa cells in the presence of 0.05 mM DNIC with thiosulfate in Versene's solution or 0.2 mM DNIC with glutathione in Eagle's medium. Ordinate: number of cells (in rel. units) [51].

corresponding to the diploid (2c) structure of DNA (Figure 2), top-22-h incubation of HeLa cells in Eagle's medium). After incubation in the presence of DNIC with thiosulfate in 0.5 mM Versene's solution (ethylenediamine tetra acetate, EDTA), which normally initiates DNIC-Thiosulfate decomposition, the population of apoptotic cells increased significantly with the DNIC concentration (Figure 2), bottom, left graph). A similar effect was observed after incubation of HeLa cells with DNIC-Glutathione + Bathophenanthroline Disulfonate (BPDS) (Figure 2), bottom, central graph). Another NO donor, GS-NO, initiated apoptosis in HeLa cells in the absence of iron chelators (Figure 2, bottom, right), most probably, as a result of fast spontaneous decomposition of GS-NO and a concomitant release of considerable amounts of NO, which manifested strong apoptotic activity against HeLa cells. It may be inferred from these data [51] that in the course of their decomposition by iron chelators DNIC exert a cytotoxic effect on HeLa cells. This finding led us to suppose that the cytotoxic activity of DNIC is manifested in the presence of endogenous iron chelators generated by rapidly proliferating cells and tissues in order to supply the latter with iron essential for their normal growth. Obviously, after incubation of cells and tissues with DNIC the latter can undergo decomposition by endogenous iron chelators; the iron released thereupon is utilized for maintaining the vital activity of biological objects. This reaction is accompanied by a release, from the decomposing DNIC, of large amounts of NO, which were further converted into cytotoxic peroxynitrite. Such is the mechanism that may be responsible for the selectivity of cytotoxic effects on DNIC on rapidly proliferating cells and tissues, e.g., on cells of non-malignant, e.g., endometrioid, tumors. These findings suggest that exogenous DNIC with thiol-containing ligands simulate both beneficial (regulatory) and cytotoxic effects of endogenously produced NO. As, judging from the most recent data [14,15], these DNIC are formed in animal tissues and cell cultures as major products in the presence of endogenous NO, they have every right to be regarded as a "working form" of endogenous NO, which determines their functional activity. It is this particular form of NO that is responsible for the suppression of growth of endometrioid tumors in animals and man. Conclusive evidence in favor of this conclusion is given below.

A Model of Surgically Induced Experimental Endometriosis in Rats: Benefits and Pitfalls

A model of surgically induced experimental endometriosis in rats, which included transplantation of two fragments of uterine tissue (2 x 2 mm) onto the inner surface of the abdominal wall, was used as a model of choice in our studies. The experiments were carried out on adult female Wistar rats weighing 160 to 180 g supplied by the "Stolbovaya" Affiliated Nursery of the Russian Academy of Medical Sciences. Throughout the 45-day observation period, the animals were housed at the vivarium of the N.M. Emanuel Institute of Biochemical Physics of the Russian Academy of Sciences, in full compliance with the Guidelines of the Geneva Convention "International Principles for Biomedical Research Involving Animals" (Geneva, 1990).

Protocol: Induction of experimental endometriosis

Experimental endometriosis was simulated in rats using a modified surgical procedure described by Vernon and Wilson [52]. All the animals were at the proestrus stage of the estrous cycle. Surgical manipulations were performed in the supine position on a standard

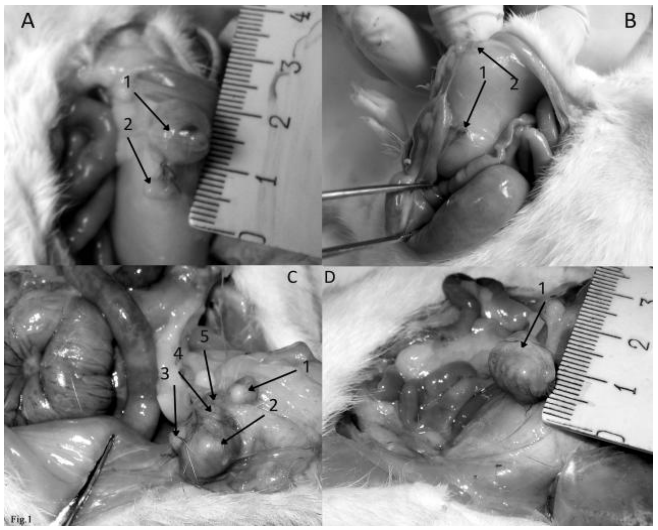

Figure 3: The representative photo images of abdominal tissue samples of experimental (B and D) and control (A and C) rats (Groups 1 and 2). The positions of EMT on panels A, C and D are indicated by arrows 1 and 2; on panel B, EMT are absent (the endometrial implant niduses are indicated by arrows 1 and 2). On panel C, additive small-size tumors are indicated by arrows 3-5 [2].

rat surgery board under thiopental anesthesia (0.06 g/kg wt) with xylazine (3 mg/kg wt) premedication and lasted 40-45 min. Tumor growth was induced by surgical transplantation of two autologous fragments (2 x 2 mm) of uterine tissue (the endometrium together with the myometrium) excised from the left uterine horn onto the anterior surface of the abdominal wall. After termination of invasive treatment, the rats were kept for 4 days under standard vivarium conditions (controlled environment, constant temperature (23±2°C, 12-h light/dark cycles). Standard dietary intake including free access to water was used to accelerate the engraftment. The use of rodents (e.g. rats) for simulating endometriosis in experimental animals has pros and cons of its own. To obvious merits, one can relate their low cost, easy maintenance (in comparison with, e.g. primates) and a relatively short (4-5 days) and frequent (70-80 cycles per year) estrous cycle (cf. 12 cycles in primates). Moreover, rodents are distinguished for long-lasting (2 years) reproductive activity enabling the monitoring of various impacts of simulated endometriosis on the reproductive cycle and to follow the progress of impregnation, gestation and delivery [53], and last but not least, surgical manipulations (including surgically induced endometriosis) are tolerated by rodents more easily than by primates. The main pitfall of simulating endometriosis in rodents is their remote position on the evolutional scale relative to primates whose physiology is the closest to that of human beings. Rodents have no menses [54], so their endometrium is not subject to menstrual exfoliation. However, the extracellular matrix of the rodent uterus is highly susceptible to proteolysis depending on the collagen content in their excrements [55].

B-DNIC with Glutathione Suppress the Development of Surgically Induced Endometriosis in Rats

As stated earlier in this paper, in this study experimental endometriosis was simulated in rats by transplantation of two small

Table 2: The results of statistic evaluation of the mean volumes of EMT (in mm^3) (overall data for all animals) [2].

	Median (min-max)	Mean±SEM
Group 1		
Control rats (n = 10)	36 (2–599)	113±179
Experimental rats (n = 10	0 (0–73)	7±17 p<0.001
Group 2		
Control rats (n = 10)	30 (2–866)	150±230
Experimental rats (n = 10)	7 (0–759)	106±23 p<0.008

(2-mm) fragments of uterine tissue onto the inner surface of the abdominal wall. Thirty to forty-five days after surgery, the implants developed into large-size (≤ 1 cm) oval-shaped Endometrioid Tumors (EMT) (Figure 3A and 3C); their growth ceased gradually during 2 months after surgery.

Four days after surgery, Group 1 rats were given an intraperitoneally dose of B-DNIC with glutathione (6.25 μmoles/kg or 12.5 μmoles as calculated per one iron atom in B-DNIC). The treatment course included one daily injection of B-DNIC and lasted 10 days with subsequent two-week keeping of animals on a standard vivarium diet. After completion of treatment, EMT failed to be detected in the majority of experimental rats (Figure 3B) (Table 2), while in the control group large-size EMT (mean volume ≤ 110 mm^3) continued to develop throughout the observation period (30 days) (Figure 3A) (Table 2).

In Group 2 rats, B-DNIC injections (12.5 μmoles/kg daily, for 10 days) were begun on day 30 after surgery, when the growth of large-size tumors was complete, and were performed daily, for 10 days. In the subsequent period, the animals were kept on a standard vivarium diet for another 4–5 days. In these rats, the growth of EMT estimated on day 45 after surgery appeared to be suppressed; several animals displayed the presence of only one (instead of two) tumor (Figure 3D). It is noteworthy that the mean size of EMT was essentially the same as that in Group 1 rats (control) estimated one month after surgery (Table 2, lines 1 and 4). Control rats of Group 2 displayed the presence of two large-sizes EMT; their mean volume estimated 1.5 months after surgery was 150 mm^3. Several animals of this group had multiple small-size additive tumors (Figure 3C). In B-DNIC-treated experimental rats of Group 2, additive tumors were absent. The histopathological analysis of large-size EMT established complete lack of uterine endometrial cells responsible for tumor growth [54]. Judging from the data obtained, DNIC can indeed suppress the growth of rapidly proliferating EMT in full conformity with the aforesaid hypothesis. In experimental rats treated with the Fe^{2+} + glutathione mixture instead of B-DNIC with glutathione, the cytotoxic effect on EMT growth failed to be established [2]. Apparently, the inhibiting effect of B-DNIC with glutathione on tumor growth must be attributed to their nitrosyl ligands rather than to glutathione and bivalent iron. In the framework of the hypothesis on the role of endogenous iron chelators in the decomposition of B-DNIC, the latter can take place either in the vicinity or in the interior of cells producing these chelators. It is this ability of rapidly proliferating cells that might determine the selectivity of the cytotoxic effect of DNIC on these cells. Indeed, in our study the cytotoxic activity of B-DNIC with glutathione was manifested only against EMT without any effect

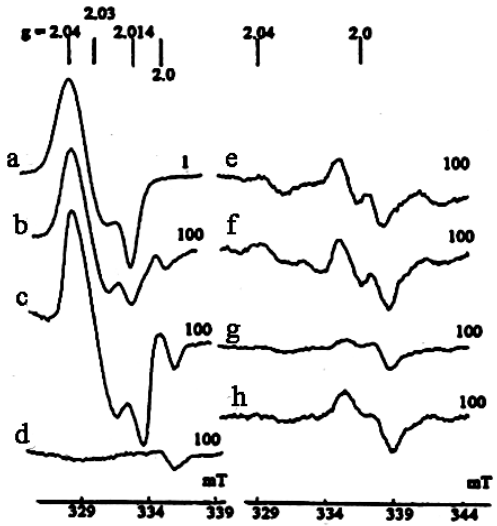

Figure 4: The representative EPR spectra recorded in EMT (a, b, e-h) and blood (c, d) samples of experimental and control rats. a, b, e - EMT samples of Group 2 rats assayed 10 min, 1 h and 24h and blood samples (c, d) assayed 1h and 24h after intraperitoneally injection of DNIC with glutathione. f, g – EMT samples of control or experimental rats of Group 2, respectively. h - EPR spectrum of the abdominal wall of Group 2 rats (control) on the side opposite to EMT. The EPR spectra of exogenous (a-c) or endogenous DNIC (e-g) (g = 2.04, 2.014) and the active form of rib nucleotide reductase (RNR) (g = 2.01, doublet splitting) were recorded at 77K. The relative amplification of the radio spectrometer is indicated to the right of the graph [2].

on neighboring organs and tissues, including the abdominal wall and the intestine. The measurements of EPR spectra in EMT samples of experimental and control rats (Group 2) revealed the following. In rats treated intraperitoneally with B-DNIC-Glu (12.5 μmoles/kg), the characteristic EPR signal of M-DNIC (the 2.03 signal) ($g_{\perp}$ = 2.04, $g_{||}$ = 2.014, $g_{aver.}$ = 2.03) [10] was recorded 10 min, 1h and 24h after injection, respectively (Figure 4A,4B, and 4E). The appearance of the paramagnetic form of DNIC in biological objects in response to the transfer of $Fe(NO)_2$ groups from diamagnetic EPR-silent B-DNIC to thiol groups of proteins culminated in the formation of protein-bound M-DNIC. Evidence for their protein origin can be derived from the preservation of the anisotropic shape of their EPR signals with the increase in the registration temperature from 77K to ambient temperature (for explanation see [10]).

The intensity of the 2.03 signal (Figure 4A) recorded 10 min after treatment of rats with B-DNIC corresponded to 500 nmoles of M-DNIC per two EMT. After 1h, the signal intensity diminished to 6 nmoles of M-DNIC per two EMT with a further drop to 1 nmole per two EMT on the next day (Figure 4B and 4E). The 2.03 signal with the mean intensity corresponding to 1 nmole per two EMT was also recorded in EMT of control animals of both groups (Figure 4F). In addition, these EMT produced an EPR signal with doublet (2.3 mT) splitting at g = 2.01 characteristic of the active form of Rib Nucleotide Reductase (RNR) [56]. The intensity of the EPR signal in EMT of experimental rats of both groups was three times lower than in control (Figure 4G). Noteworthy, an intense EPR signal corresponding to the active form of RNR was recorded in samples of abdominal wall tissue on the side opposite to EMT (Figure 4H). A 2.03 signal was recorded in the EPR spectra of blood samples collected 1h after treatment of rats

Table 3: Statistic estimation of the total mean volume of EMT (in mm^3) [3].

Animals	Median (min-max	MeanS.D	p
Control (n=15)	42.4 (0–1838)	210±371	
Rats treated with DNIC (n=9)	0.0 (0–44)	5±7	0.0001
Rats treated with GS-NO (n=9) (without regard for oversize tumors)	12.6 (0–339)	51±76	>0.1
Rats treated with GS-NO (n=9) (with regard for oversize tumors)	28.8 (0–25282)	1392±4916	>0.6

with B-DNIC (Figure 4C); its intensity corresponded to the M-DNIC concentration of 8 nmoles/ml of blood. However, no such signal was detected on the next day after B-DNIC treatment (Figure 4D). These results suggest that 1h after treatment of control rats with B-DNIC with glutathione the concentration of protein-bound M-DNIC formed in their EMT was by two orders of magnitude less than that determined 10 min after B-DNIC treatment (500 *vs.* 6 nmoles per two EMT), which testifies to the fast decomposition of DNIC and the appearance of significant amounts of NO in EMT samples. Further oxidation of the latter to cytotoxic peroxynitrite seems to be the most probable reason for the suppression of EMT growth in experimental rats. Noteworthy, this effect is selective and valid for EMT only.

The detection of M-DNIC in EMT samples of control (non-treated with exogenous B-DNIC) rats testifies to activation of the system responsible for the NOS-induced synthesis of endogenous NO in abdominal tissues of experimental rats. However, the steady-state concentration of NO in these EMT samples appeared to be significantly lower in comparison with the initial concentration of exogenous NO measured within the first 10 min after treatment of animals with exogenous B-DNIC (1 *vs.* 500 nmoles per two EMT), as could be judged from the concentration of M-DNIC formed thereupon. In all probability, this difference determines the magnitude of the cytotoxic effect of exogenous B-DNIC on EMT. The time-dependent drastic decrease of the M-DNIC concentration in EMT may be attributed to the transfer of the bulk of exogenous DNIC from abdominal tissues to circulating blood. Indeed, one hour after treatment of rats with B-DNIC, the M-DNIC were detected in animal blood at the concentration of 8 nmoles/ml. Considering that the volume of the circulating blood did not exceed 10–15 ml, the concentration of M-DNIC in whole blood was equal to 100 nmoles, which was significantly less than that measured in EMT samples 10 min after B-DNIC treatment (500 nmoles per two EMT or the total dose of B-DNIC (2.5 μmoles per rat) as calculated per one iron atom in B-DNIC). These data are strongly suggestive of the drastic time-dependent decrease of M-DNIC in EMT samples in response to the decomposition of B-DNIC in the vicinity of EMT. The detection of an EPR signal (g = 2.01, doublet splitting) corresponding to the active form of Rib Nucleotide Reductase (RNR) [56] was another important finding of this study. The appearance of a form responsible for DNA synthesis suggested enhanced proliferation of EMT in control animals [56]. Judging from the intensity of its EPR signal, the concentration of the active form of RNR in the group of experimental rats diminished, which is consistent with the inhibiting effect of B-DNIC on EMT. Interestingly, the EPR signal corresponding to the active form of RNR was recorded on the opposite (with respect to EMT) side of the abdominal wall, where EMT were absent. This finding points to a high proliferative activity of abdominal tissue at large and may be responsible for the appearance of small-size additive EMT in control rats (Group 2). The effects of other NO donors (e.g., S-nitrosothiols) on the development of endometriosis were found to be different from those of DNIC. The same group of Mexican investigators established [57] that prolonged (for several months) treatment of mice with surgically induced endometriosis with the S-nitrosothiol derivative S-nitrosopenicillamine (SNAP) used at a much lower (in comparison with DNIC) doses significantly enhanced the EMT growth instead of suppressing it. The immune status of SNAP-treated rats estimated by interleukin and interpheron content appeared to be notably decreased suggesting enhanced proliferation of EMT. Similar results were obtained in experiments on GS-NO-treated rats [3]. In this case, the effect of GS-NO on rats with surgically induced endometriosis was studied using the same protocol as in experiments on DNIC-Glu-treated rats where GS-NO (12.5 μmoles) was injected beginning with day 4 after surgery; the treatment course lasted 10 days and included 10 injections. In parallel studies, this protocol was used for the treatment of Group 1 rats with DNIC with glutathione. As in our previous studies [2], treatment of experimental rats with B-DNIC (12.5 μmoles/kg calculated per one iron atom; daily, for 10 days) with subsequent keeping on a standard vivarium diet over a period of two weeks culminated in complete suppression of EMT growth (Figure 5) (Table 3). In 6 out of 9 animals, EMT were absent, while in the rest (n = 3) their mean volume did not exceed 5 mm^3.

In addition to large-size tumors grown from uterine tissue

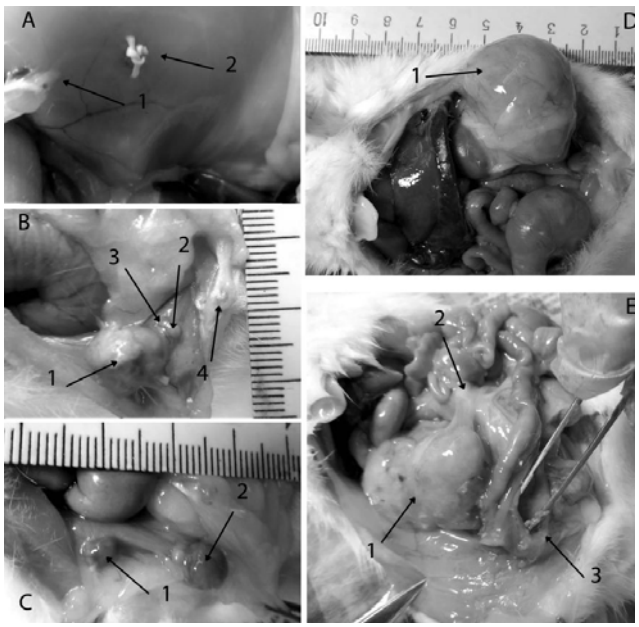

Figure 5: The representative photoimages of tissue samples of DNIC-treated (A), control (B) and GS-NO-treated rats (C-E). (D,E) GS-NO-treated rats with oversize EMT. The positions of EMT on panels A-D are marked by arrows 1 and 2. Panel B- additive small-size tumors (arrows 3 and 4). Panel E - arrows 1-3 indicate EMT [1], multiple adhesions in the intestine (2) and the area of massive dissemination of the abdominal wall with germinal tumors (3) [3].

Table 4: The mean size of EMT calculated per one animal (in mm^3) [3].

Animals	Median (min-max)	Mean±S.D	p
Control rats (n=15)	393 (26–2449)	534 ±620	
Rats treated with DNIC (n=9)	0 (0–55)	10±19	0.0003
Rats treated with GS-NO (n=9) (without regard for oversize tumors)	130 (0–431)	161±150	0.0005
Rats treated with GS-NO (n=9) (with regard for oversize tumors)	207 (0–25348)	4641±8472	>0.002

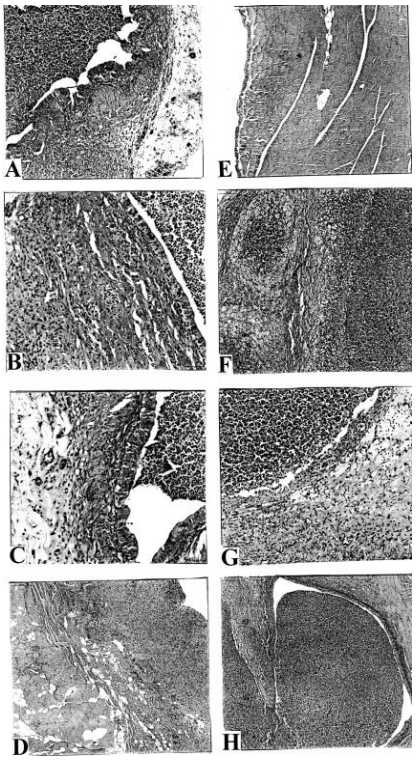

Figure 6: A histopathological view of EMT tissues of control (A-C), DNIC-treated (D,E) and GS-NO-treated rats (F-H). (A-C) The auto graft represents an enlarged cystic endometrial gland with multiple small-size glandules. The lumen is filled with neutrophilic granules. The endometrial stroma is active and is infiltrated with neutrophils. (D,E) The endometriotic niduses display a complete lack of endometrial glands, which are replaced by fibrous tissue and contain collagen depots and granulation tissue of different degrees of maturity. (F,C) The tissue samples of small-size tumors contain large endometriotic cysts with debris along the polymorph nuclear elements suggestive of inflammation. Congestions of foamy macrophages are visible on the periphery of endometrial lesions. Such patterns are characteristic of oversize tumors (H). The macrophagial response is absent [3].

implants, all control rats (n = 15) had multiple small-size additive tumors (Figure 5B) (n = 38). In all GS-NO-treated animals of this group (n = 9), the total number of EMT (including those developed from tissue implants plus additive tumors) was 30. Oversize's EMT were detected in 3 rats and were localized in the implant niduses. Their size exceeded that in the control group by one or two orders of magnitude. Without regard for oversize tumors, the mean size of EMT in GS-NO-treated rats was 51±76 mm^3, i.e., it exceeded the control value fourfold (Table 3). With regard to oversize tumors, the mean tumor size exceeded that in the control group sevenfold (1392±4916 mm^3). Similar results were obtained when these data were recalculated per one animal (Table 4).

The histopathological data suggest that despite the obvious retardation (in comparison with control) of the EMT growth in the majority of GS-NO-treated rats, their EMT contained significant amounts of endometrial cells responsible for tumor growth. Their histological characteristics were similar to those in control animals (Figure 6).

These data altogether indicate that GS-NO do not exert a beneficial effect on the development of experimental endometriosis in rats. The slow growth of endometrioid tumors in GS-NO-treated rats can be attributed to the presence of multiple adhesions in the abdominal cavity (Figure 5E), which prevent vascularization of EMT and, as a consequence, suppress their proliferation. If for one reason or another this does not take place, the growth of EMT continues, culminating in the appearance of oversize tumors.

Interesting results were obtained during an EPR analysis of tissue samples of rats with EMT (Figure 7). The EPR spectra of EMT samples of control and GS-NO-treated rats recorded in the final steps of these experiments displayed the presence of EPR signals corresponding to the active form of RNR, namely, a doublet EPR signal with a peak at g = 2.01 and a 2.03 signal (Figure 7A and 7B). The former is characteristic of rapidly proliferating tissues [56] and may be considered as a marker of enhanced proliferation of EMT, while the latter testifies to the enhanced production of NO. Quite probably, this phenomenon represents a specific response of the immune system, where the suppression of tumor growth is manifested in enhanced production of cytotoxic NO by immunocompetent cells. The detection, in several EMT samples, of an intense EPR signal of nitrosyl hemoglobin complexes (Figures 7D and 7E) provides conclusive evidence for this hypothesis. It is noteworthy that none of the tissue samples obtained from DNIC-treated rats with small-size EMT were able to generate these EPR signals, with the exception of a weak EPR signal produced

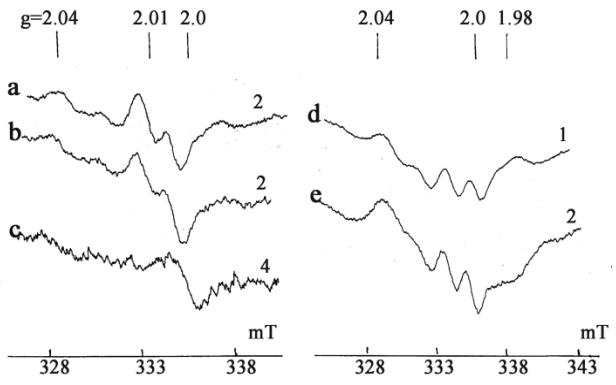

Figure 7: The representative EPR spectra of the endogenous paramagnetic centers recorded in EMT samples of control (a,b) and GS-NO-treated (b,e) rats at 77K. The EPR signal (c) is assigned to the free-radical centers in a tissue sample of a DNIC-treated rat, consisting of a small-size EMT and surrounding abdominal tissues [3].

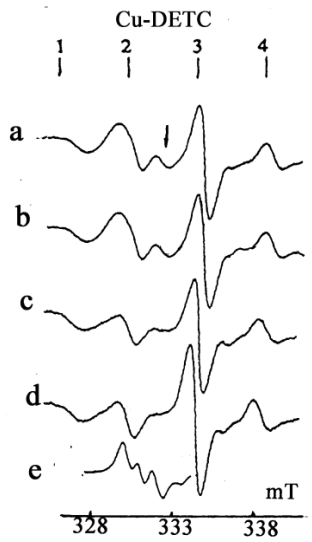

Figure 8: The representative EPR spectra recorded in EMT samples of control (a) and GS-NO-treated rats (b), in a tissue sample of a DNIC-treated rat consisting of small-size EMT and surrounding tissues (c) and in abdominal tissue samples of an intact rat without endometriosis (d). All the animals were treated with Fe^{2+}-DETC as a NO trap. (e) - The EPR signal of MNIC- DETC. (Lines 1-4) -The four components of the hyperfine structure (HFS) of the EPR signal of Cu^{2+}-DETC complexes. The high-field component of the triplet HFS of the EPR signal of MNIC-DETC is indicated by an arrow (a). All the EPR spectra were recorded at 77K [3].

by endogenous free radicals at g = 2.0 (Figure 7C).

The formation of endogenous NO in EMT samples of control and GS-NO-treated rats was also observed during incorporation of NO into the spin trap Fe^{2+}-Diethyldithiocarbamate (DETC) and was manifested in the appearance of EPR signals of mononitrosyl iron complexes with DETC (MNIC-DETC) [58]. The spin trap was administered to animals one hour prior to sacrifice. Treatment of rats with and without EMT with B-DNIC was carried out using a similar protocol. Previously, it was found [58] that the characteristic EPR signal of MNIC-DETC recorded at 77K ($g_{\perp}$ = 2.045; $g_{||}$ = 2.02) had a triplet Hyperfine Structure (HFS) with splitting at 1.2 mT (Figure 8E). In all cases studied, this signal overlapped with the characteristic EPR signal of DETC complexes with endogenous Cu^{2+}, which had a four-component HFS (Figure 8, lines 1–4) [58]. The appearance of an EPR signal of MNIC-DETC against the background of the intense EPR signal of Cu^{2+}-DETC was detected by the third (high-field) component of the triplet HFS in the EPR signal of MNIC-DETC (Figure 8A and 8B). This component is specific to NO synthesis and was present in the EPR spectra of EMT samples of both control and GS-NO-treated rats (Figure 8A and 8B), but not in the EPR spectra of B-DNIC-treated rats and of rats without EMT (Figure 8C and 8d).

Judging from the intensity of this component, about 1–2 nmoles of NO per two EMT were incorporated into MNIC-DETC of control and GS-NO-treated rats, which is commensurate with the concentration of M-DNIC in EMT tissues of experimental animals (Figure 7A and 7B). These data provide additional evidence that in EMT tissues DNIC with thiol-containing ligands are predominantly represented by the M-form. A similar ratio between the M- and B-forms of endogenous DNIC was established in experiments with cultured isolated animal cells [14,59].

The results of yet another series of our experiments where GS-NO was used as a NO donor are in perfect agreement with those obtained by the Mexican team [57], viz., in contrast to DNIC with thiol-containing ligands, S-nitrosothiols were not only incapable to suppress the development of experimental endometriosis in rats, but even stimulated further growth of EMT. Therefore, it would be reasonable to suppose that the cytotoxic effect of S-nitrosothiols after their chronic administration to rats was provided by their fast decomposition and was accompanied by a release of considerable amounts of NO. These events are prerequisite to the appearance, in the animal organism, of significant amounts of cytotoxic peroxynitrite formed in response to the NO interaction with superoxide anions.

Similar to the cytotoxic effect of SNAP reported by the Mexican investigators [57], high cytotoxic activity of GS-NO, which in our studies manifested itself in the deterioration of the immune status of experimental rats, might be due to the fact that the decomposition of both S-nitrosothiols affected not only the tissues surrounding EMT, but involved the whole mass of the abdominal tissue. Correspondingly, the cytotoxic effect of S-nitrosothiols might be directed not only against EMT, but also against other tissues. As regards the cytotoxic effect of DNIC, it might result from their decomposition either inside or in the vicinity of EMT. In the framework of this hypothesis, which has every chance to be plausible, such decomposition is initiated by the release, from rapidly proliferating EMT, of iron chelators able to initiate the decomposition of DNIC and the appearance of significant amounts of NO and cytotoxic peroxynitrite responsible for the selective apoptosis of EMT.

DNIC with Glutathione Attenuate Pain Attacks in Rats with Experimental Endometriosis

In women, the main manifestations of endometriosis include low impregnation capacity and a variety of pain syndromes, e.g., severe dysmenorrhea (excessive menstrual pains), severe dyspareunia (pelvic pain during sexual intercourse), dyschesia (menses-related pelvic pains upon defecation) and chronic pelvic pains. In some females, the pain syndrome is concomitant with manifestations of severe chronic diseases and pain syndromes, such as irritable bowel syndrome, interstitial cystitis, and recurrent attacks of kidney stones, vulvodynia, migraine and fibromyalgias [60–63]. Chronic pelvic pains can initiate psychological disturbances, such as chronic fatigue syndrome, depression and anxiety [64]. The relationship between endometriosis and pain is still poorly understood; however, recent investigations into the nature of various pain syndromes in female patients and in animals with simulated endometriosis shed additional light upon this problem. Many aspects of the hitherto unaccountable persistence of pelvic pains after surgical removal of EMT were elucidated in a series of brilliant investigations carried out by Berkley et al. [65–68].

The role of Nitric Monooxide (NO) derivatives in neuronal processes is difficult to overestimate. Nitric oxide plays a crucial role in an immense diversity of signaling and pain processing reactions, including nociception and antinociception [69,70]. The fact that both the signaling function and the binding of NO to its specific receptors

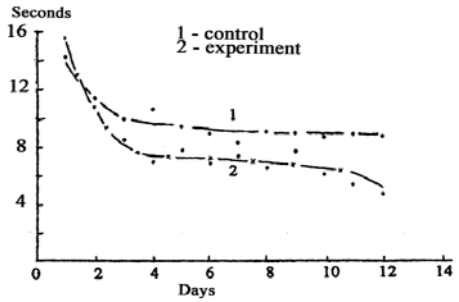

Figure 9: The changes in the mean duration of a single pain attack (in sec) in the control and experimental groups (the total duration of the observation period was 12 days). The zero point corresponds to the onset of treatment (day 28 after surgery) [74].

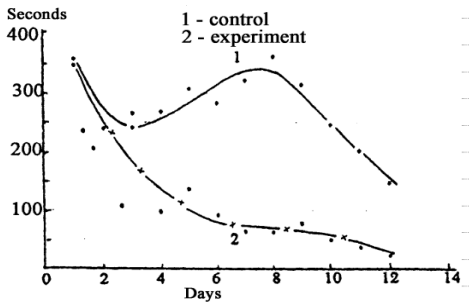

Figure 10: The changes in the total duration of the pain attacks (in sec) recorded during the 2-hour observation period. The zero point designates the onset of treatment (day 28 after surgery) [74].

Internal factors include progressive hyperalgesia resulting from additional functional innervation in endometrial implant niduses [68]. In the aforecited studies, ectopic endometrial cysts acquired elementary sensory and sympathetic innervation during the first two weeks after transplantation. During the next 3–4 weeks, these abnormalities turned to functional and become involved in neurogenic inflammation. By the end of the 4th–5th week, hyperalgesia became especially apparent due to the appearance, in the cyst interior, of a multitude of sensory and sympathetic nerve fibers.

are impossible without the involvement of free sulfhydryl groups of amino acids of high- and low-molecular-weight peptides, is now taken as evidence [71,72]. The regulatory role of sulfhydryl groups is determined by their ability to interact with NO or, more specifically, with its ionized form (NO^+) to give S-nitrosothiols that stabilize NO. This effect of NO can also be achieved through its incorporation into DNIC (see above). However, the ability of DNIC to accumulate and release NO in various pain signaling processes still remains to be elucidated.

Previous studies established that treatment of rats with surgically induced endometriosis with DNIC-glutathione strongly suppressed the further progress of the disease. It seemed, therefore, very tempting to examine to what extent these DNIC reduce pain manifestations in experimental rats. Daily 2h observations over control and experimental rats with pain syndromes were carried out simultaneously by four investigators as described in [52]. The animals were kept in individual cages (one animal per cage) located at a reasonable distance from one another. Selection of animals was performed on a random principle; each rat was in the proestrus phase. To minimize the impact of individual factors, the groups of animals (control – experiment) changed every day. The duration of posture-related pain manifestations [73] was measured with the help of a stop-watch.

Figures 9 and 10 illustrate the changes in the mean duration of a single pain attack and the total duration of the pain attacks during the observation period (2h) (mean data from 4 animals) [74]. From Figure 9 it follows that the mean duration of a single pain attack in DNIC-treated and control rats diminished with time. The faster decrease in this parameter in the experimental group pointed to the antinociceptive activity of DNIC. Estimation of the total duration of pain attacks within a 2h observation period gave similar results (Figure 10).

These studies also demonstrated that the mean duration of a single pain attack in control rats increased on day 36 after surgery on day 8 after the onset of treatment), which can be assigned to the influence of external and internal factors. The former include drastic fluctuations in atmospheric pressure, which has strong impacts on the behavioral activity of experimental animals, and, possibly, estrous variations not established by the experimenters. (On the other hand, fluctuations of atmospheric pressure are known to exert similar effects on both experimental and control animals).

It is not excluded that similar changes in the density of nerve fibers in endometrial implant niduses and, consequently, the increase in the overall duration of the pain attacks on week 5 after surgery also took place in control rats. In the experimental group, the monotonous decrease of these parameters was suggestive of the depletion of endogenous NO generated by the constitutive forms of NO synthesis by virtue of their inability to produce the antinociceptive effect. It may thus be concluded that administration of NO within a complex with reduced thiols opens up fresh opportunities for relieving pain manifestations in animals and man.

B-DNIC with Glutathione Suppress the Proliferation of Transplanted Lewis Lung Carcinoma Cells in Early Steps of Tumor Growth in Mice

The discovery of selective cytotoxic effects of B-DNIC with glutathione on cells of non-malignant Endometrioid Tumors (EMT) prompted the idea to investigate their activity against rapidly proliferating malignant tumors. The very first studies in this area established that daily intraperitoneal infusions of B-DNIC with glutathione to mice bearing Lewis lung carcinoma for 10 days can indeed inhibit the growth of this subcutaneous tumor in a dose-dependent manner, however, only in the initial steps of tumor development. In the subsequent periods, tumor growth continued at the same or even higher rates in comparison with control (Figure 11) [75].

Interestingly, simultaneous treatment of rats with B-DNIC with glutathione and a 10-fold excess of free glutathione notably enhanced the cytotoxic effect of B-DNIC on Lewis carcinomas (Figure 11), most probably, due to the high concentration of low-molecular DNIC in animal blood. In the absence of free glutathione, the greater part of DNIC was bound to proteins as a result of which the cytotoxic effect of DNIC on tumor growth was significantly attenuated.

These findings suggest that despite their high cytotoxic activity

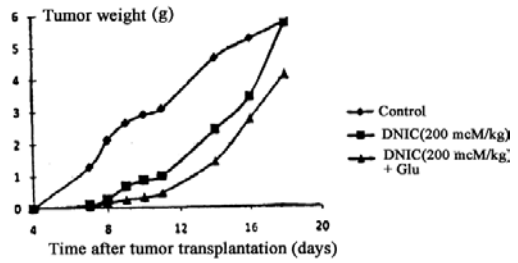

Figure 11: The changes in the mass of Lewis carcinomas in control mice and in mice treated with B-DNIC-Glu or B-DNIC-Glu + free glutathione (0.2 mM and 2 mM/kg, respectively) recorded on the 4th post-implantation day [75].

against non-malignant EMT, DNIC with glutathione are incapable to suppress the growth of malignant tumors. One should not rule out the possibility that malignantly transformed cells possess an ability to generate antinitrosative protection proteins attenuating the cytotoxic effect of NO or, more specifically, of peroxynitrite generated from it. In this respect, the specific response of malignantly transformed cells and tissues to the cytotoxic effect of NO is similar to that established for bacterial cells. Previous studies have demonstrated that the appearance of NO in bacterial cells initiates the expression of antinitrosative protection genes and, as a consequence, of proteins responsible for the oxidation and reduction of exogenous NO and thus decrease appreciably its concentration in bacterial cells [76]. The similarity of the specific responses of malignantly transformed and bacterial cells to NO indicates that a comprehensive search for compounds able to suppress the activity of antinitrosative protection proteins is a promising approach to suppressing the growth of malignant tumors through their treatment with NO donors, such as DNIC with thiol-containing ligands causing selective inhibition of rapidly proliferating cells and tissues.

Stipulating that in bacterial cells antinitrosative protection proteins are largely represented by heme-containing proteins or, more specifically, by heme groups responsible for the oxidation-reduction of NO, it may be conjectured that in the presence of NO excess heme groups of proteins undergo irreversible oxidation and thus become fully disabled. It is also quite probable that precisely the same events took place in our studies where fast tumor growth was recorded on day 12, i.e., immediately after cessation of DNIC treatment. If the expression of the antinitrosative protection proteins did occur at the genomic level, its activation might be initiated within one or two days after exposure of malignant cells to DNIC as a NO donor. Subsequent expression of antinitrosative protection proteins might initiate the rapid growth of Lewis carcinomas. The lack of this effect in DNIC-treated rats suggests that NO released from DNIC suppressed both the activity of antinitrosative protection proteins and the intensity of the metabolic processes occurring in malignantly transformed cells. In its turn, the resumption of protein synthesis immediately after cessation of DNIC treatment points to the release of the remainder of NO from EMT and, as a consequence, their fast proliferation. However, the results of the next series of our studies are at variance with this hypothesis, as can be evidenced from the changes in the EMT mass, which did not differ from those observed after prolonged (20-day) treatment of rats with B-DNIC (in press).

The Therapeutic Efficiency of Oxacom in the Treatment of Endometriosis in Human Patients

The hypotensive drug Oxacom designed in collaboration with a research team at RCRPC represents a dry powder obtained by lyophilization (–45°C) of 19 mM citrate-phosphate buffer (pH 7.4) containing 2.5 mM B-DNIC with glutathione, 13 mM free glutathione, 0.6 mM dextran (M_r = 40 kDa) and 0.9% NaCl. After long-term storage of the degassed preparations in hermetically sealed ampoules, the drug fully retained its physico-chemical and biological characteristics for a sufficiently long period of time (1–1.5 and more years). The weight fraction of DNIC in the dry preparation was ~ 4% [31].

As stated earlier in this chapter, Oxacom had successfully undergone clinical trials [31]. Its lethal i/v dose (LD_{50}) for mice and rats is 3500–3600 and 3200–3300 mg/kg (70–72 and 64–66 μmoles of B-DNIC with glutathione/kg), respectively. A single intravenous or chronic dose of Oxacom did not produce any appreciable effect on different cell populations of rabbit blood, while administration of the drug to mice over a period of 1–19 days was not accompanied by any manifestations of mutagenic activity either against murine bone marrow cells or on the brood and body mass of newborn rats. These animal studies demonstrated complete safety of Oxacom used at doses from 200 to 300 mg/kg (4–6 μmoles B-DNIC with glutathione per kg). Noteworthy, at the 0.5–1 μmole/kg dose B-DNIC with glutathione induced a notable (by 50%) drop of arterial pressure [31,77].

A question arises: if B-DNIC with glutathione (Oxacom) have a beneficial effect on rats with surgically induced endometriosis, will Oxacom produce a similar effect on human patients with endometriosis, one of the most rapidly progressing diseases among the female population of our planet? Our animal studies established that endometrioid tumors are non-malignant; hence, endometriosis is not a cancerous disease. Moreover, endometrioid tumors are highly sensitive to cytotoxic effects of DNIC with thiol-containing ligands. In our studies, low (≤ 6 moles/kg) doses of B-DNIC with glutathione strongly suppressed tumor growth in rats even after 10-day treatment [1-3]. But how high must the B-DNIC dose be in order to suppress EMT growth in female patients at more advanced steps of the disease? If the human dose exceeds radically the animal dose, the use of DNIC in the treatment of endometriosis in human patients is of limited utility. The reason is that high doses of DNIC exert strong hypotensive effects, which must be taken into consideration when DNIC are administered to human patients by intraperitoneal or intravaginal route. Remission of endometriosis in DNA-treated females also presents a problem, since the etiology of simulated endometriosis in animals and "natural" endometriosis in human beings is fundamentally different. In animals, surgically induced endometriosis consists in transplantation of uterine tissue grafts onto the inner surface of the abdominal wall and their subsequent development into large-size EMT. In our study, 10-day intraperitoneal treatment of rats with DNIC in the initial steps of tumor growth suppressed further development and complete resolution of EMT (the endometrial implant niduses contained only surgical threads whereby the implants had been fixed on the inner surface of the abdominal wall). Infusions

of DNIC one month after surgical transplantation fully suppressed the further growth of EMT, apparently due to the complete lack of EMT cells responsible for the fast growth of endometrioid implants (data from the histopathological analysis).

The totality of experimental data strongly suggest that remission of endometriosis in experimental animals was hardly possible, because tissue grafts did not contain any rapidly proliferating endometrial cells responsible for EMT growth. In female patients, this factor is absent and endometriosis can be invoked by transplantation of endometrial cells onto the surface of the abdominal wall. However, the factor initiating the release of endometrial cells from uterine tissue still remains to be established, since for reasons unknown the release of endometrial cells after cessation of DNIC treatment may initiate remission of endometriosis. The results obtained by a research team led by the coauthor of this review, Academician L.V.Adamyan, President of the Russian Society for Endometriosis, provide conclusive evidence that remission of endometriosis recorded in 75% of patients within two years after surgical treatment, can be assigned to the failure to remove small-size EMT in the course of the surgical procedure. Such EMT might otherwise be easily eliminated through administration of DNIC. As far as remission is concerned, it may be related to the extraordinarily high susceptibility of some female patients to endometriosis and this fact should not in any way be neglected.

It remains to be hoped that the problem of remission and related problems will soon be overcome through a comprehensive analysis of direct effects of DNIC on human patients.

Acknowledgement

This work has been supported by the Russian Foundation for Basic Research (Grant No 15-04-00708a) and the Presidium of the Russian Academy of Sciences (Program "Fundamental Sciences to Medicine, 2014).

References

1. Burgova EN, Tkachev NA, Vanin AF. [The dinitrosyl-iron complexes with cysteine block the development of experimental endometriosis in rats]. Biofizika. 2012; 57: 105-109.
2. Burgova EN, Tkachev NĐ, Adamyan LV, Mikoyan VD, Paklina OV, Stepanyan AA, et al. Dinitrosyl iron complexes with glutathione suppress experimental endometriosis in rats. Eur J Pharmacol. 2014; 727: 140-147.
3. Burgova EN, Tkachev NĐ, Paklina OV, Mikoyan VD, Adamyan LV, Vanin AF. The effect of dinitrosyl iron complexes with glutathione and S-nitrosoglutathione on the development of experimental endometriosis in rats: a comparative studies. Eur J Pharmacol. 2014; 741: 37-44.
4. Ignarro LJ. Nitric Oxide: Biology and Pharmacology. San-Diego: Acad. 2000.
5. Radi R, Denicola A, Alvarez B, Ferrer-Sueto G, Rubbo H. The biological chemistry of peroxynitrite. Ignarro L, editor. In: Nitric Oxide: Biology and Pharmacology. Acad. Press. 2000; 231-237.
6. Nathan C, Shiloh MU. Reactive oxygen and nitrogen intermediates in the relationship between mammalian hosts and microbial pathogens. Proc Natl Acad Sci U S A. 2000; 97: 8841-8848.
7. Vanin AF. Dinitrosyl iron complexes and S-nitrosothiols are two possible forms for stabilization and transport of nitric oxide in biological systems. Biochemistry (Mosc). 1998; 63: 782-793.
8. Suryo Rahmanto Y, Kalinowski DS, Lane DJ, Lok HC, Richardson V, Richardson DR. Nitrogen monoxide (NO) storage and transport by dinitrosyl-dithiol-iron complexes: long-lived NO that is trafficked by interacting proteins. J Biol Chem. 2012; 287: 6960-6968.
9. Chiang CY, Darensbourg MY. Iron nitrosyl complexes as models for biological nitric oxide transfer reagents. J Biol Inorg Chem. 2006; 11: 359-370.
10. Vanin AF, Poltorakov AP, Mikoyan VD, Kubrina LN, Burbaev DS. Polynuclear water-soluble dinitrosyl iron complexes with cysteine or glutathione ligands: electron paramagnetic resonance and optical studies. Nitric Oxide Biol. Chem. 2011; 23: 136-149.
11. Harrop TC, Song D, Lippard SJ. Interaction of nitric oxide with tetrathiolato iron(II) complexes: relevance to the reaction pathways of iron nitrosyls in sulfur-rich biological coordination environments. J Am Chem Soc. 2006; 128: 3528-3529.
12. Lo FC, Chen CL, Lee CM, Tsai MC, Lu TT, Liaw WF, et al. A study of NO trafficking from dinitrosyl-iron complexes to the recombinant E. coli transcriptional factor SoxR. J Biol Inorg Chem. 2008; 13: 961-972.
13. Lewandowska H, Kalinowska M, Brzóska K, Wójciuk K, Wójciuk G, Kruszewski M. Nitrosyl iron complexes--synthesis, structure and biology. Dalton Trans. 2011; 40: 8273-8289.
14. Hickok JR, Sahni S, Shen H, Arvind A, Antoniou C, Fung LW, et al. Dinitrosyliron complexes are the most abundant nitric oxide-derived cellular adduct: biological parameters of assembly and disappearance. Free Radic Biol Med. 2011; 51: 1558-1566.
15. Vanin AF, Mikoyan VD, Kubrina LN, Borodulin RR, Burgova EN. Mono- and binuclear dinitrosyl iron complexes with thiol-containing ligands in diverse biological systems. Biofizika (Rus). 2015.
16. Vanin AF, Burbaev DSh. Electronic and spatial structures of water-soluble dinitrosyl iron complexes with thiol-containing ligands underlying their ability to act as nitric oxide and nitrosonium ion donors. J Biophys. 2011; 2011: 878236.
17. Vanin AF, Malenkova IV, Serezhenkov VA. Iron catalyzes both decomposition and synthesis of S-nitrosothiols: optical and electron paramagnetic resonance studies. Nitric Oxide. 1997; 1: 191-203.
18. Vanin AF, Papina AA, Serezhenkov VA, Koppenol WH. The mechanisms of S-nitrosothiol decomposition catalyzed by iron. Nitric Oxide. 2004; 10: 60-73.
19. Bonner ET, Stedman G. The chemistry of nitric oxide and redox-related species. Feelisch M, Stamler JS, editors. In: Methods of Nitric Oxide Research. N-Y: John Willey& Sons. 1996; 3-18.
20. Enemark JH, Feltham RD. Principles of structure, bonding, and reactivity for metal nitrosyl. Coordination Chemistry Reviews. 1974; 13: 339-406.
21. Borodulin RR, Kubrina LN, Mikoyan VD, Poltorakov AP, Shvydkiy VO, Burbaev DSh, et al. Dinitrosyl iron complexes with glutathione as NO and NO^+ donors. Nitric Oxide. 2013; 29: 4-16.
22. Murad F. Discovery of some of the biological effects of nitric oxide and its role in cell signaling. Biosci Rep. 2004; 24: 452-474.
23. Stamler JS, Simon DI, Osborne JA, Mullins ME, Jaraki O, Michel T, et al. S-nitrosylation of proteins with nitric oxide: synthesis and characterization of biologically active compounds. Proc Natl Acad Sci U S A. 1992; 89: 444-448.
24. Harrop TC, Song D, Lippard SJ. Reactivity pathways for nitric oxide and nitrosonium with iron complexes in biologically relevant sulfur coordination spheres. J Inorg Biochem. 2007; 101: 1730-1738.
25. McDonald CC, Philips WD, Mower HF. An electron spin resonance study of some complexes with iron, nitric oxide and anionic ligands. J. Am. Chem. Soc. 1965; 87: 3319-3326.
26. Borodulin RR, Kubrina LN, Shvydkiy VO, Lakomkin VL, Vanin AF. A simple protocol for the synthesis of dinitrosyl iron complexes with glutathione: EPR, optical, chromatographic and biological characterization of reaction products. Nitric Oxide. 2013; 35: 110-115.
27. Kleschyov AL, Mordvintcev PI, Vanin AF. Nitric oxide and iron participation in hypotensive action of nitrosyl iron complexes with various anionic ligands. Studia Biophys. 1985; 105: 93-102.
28. Mordvintsev PI, Putintsev MD, Galagan ME, Oranovskaia EV, Medvedev OS. [Hypotensive activity of dinitrosyl complexes of iron and proteins in anesthetized animals]. Biull Vsesoiuznogo Kardiol Nauchn Tsentra AMN SSSR. 1988; 11: 46-51.

29. Galagan ME, Oranovskaia EV, Mordvintsev PI, Medvedev OS, Vanin AF. [Hypotensive effect of dinitrosyl iron complexes in experiments on waking animals]. Biull Vsesoiuznogo Kardiol Nauchn Tsentra AMN SSSR. 1988; 11: 75-80.

30. Vedernikov YP, Mordvintcev PI, Malenkova IV, Vanin AF. Similarity between the vasorelaxing activity of dinitrosyl iron cysteine complexes and endothelium-derived relaxing factor. Eur J Pharmacol. 1992; 211: 313-317.

31. Chazov EI, Rodnenkov OV, Zorin AV, Lakomkin VL, Gramovich VV, Vyborov ON, et al. Hypotensive effect of Oxacom® containing a dinitrosyl iron complex with glutathione: animal studies and clinical trials on healthy volunteers. Nitric Oxide. 2012; 26: 148-156.

32. Mordvintsev PI, Rudneva VG, Vanin AF, Shimkevich LL, Khodorov BI. [Inhibition of platelet aggregation by dinitrosyl iron complexes with low molecular weight ligands]. Biokhimiia. 1986; 51: 1851-1857.

33. Kuznetsov VA, Mordvintsev PI, Dank EKh, Iurkiv VA, Vanin AF. [Low molecular weight and protein dinitrosyl complexes of non-heme iron as inhibitors of platelet aggregation]. Vopr Med Khim. 1988; 34: 43-46.

34. Arkhipova MA, Mikoian VD, Vanin AF. [Effect of exogenous donors of nitric oxide and inhibitors of its enzymatic synthesis on experimental ischemic thrombosis in conjunctive veins of the rabbit eyes]. Biofizika. 2008; 53: 315-325.

35. Shirinsky VP, Kapelko VI, Vanin AF. Antihypoxic drug. Patent of Russian Federation No 252953 from June 14, 2013.

36. Shamova EV, Bichan OD, Drozd ES, Gorudko IV, Chizhik SA, Shumaev KB, et al. [Regulation of the functional and mechanical properties of platelet and red blood cells by nitric oxide donors]. Biofizika. 2011; 56: 265-271.

37. Shekhter AB, Serezhenkov VA, Rudenko TG, Pekshev AV, Vanin AF. Beneficial effect of gaseous nitric oxide on the healing of skin wounds. Nitric Oxide. 2005; 12: 210-219.

38. Shekhter AB, Rudenko TG, Serezhenkov VA, Vanin AF. [Dinitrosyl-iron complexes with cysteine or glutathione accelerate skin wound healing in animals]. Biofizika. 2007; 52: 539-547.

39. Remizova MI, Kochetygov NI, Gerbout KA, Lakomkin VL, Timoshin AA, Burgova EN, et al. Effect of dinitrosyl iron complexes with glutathione on hemorrhagic shock followed by saline treatment. Eur J Pharmacol. 2011; 662: 40-46.

40. Andreyev-Andriyevsky AA, Mikoyan VD, Serezhenkov VA, Vanin AF. Penile erectile activity of dinitrosyl iron complexes with thiol-containing ligands. Nitric Oxide. 2011; 24: 217-223.

41. Pisarenko OI, Serebriakova LI, Tskitishvili OV, Studneva IM, Vanin AF, Chazov EI. [Cardioprotective efficacy of dinitrosyl iron complex with L-cysteine in rats in vivo]. Izv Akad Nauk Ser Biol. 2008; : 110-114.

42. Serezhenkov VA, Kalinina EV, Glazunova VA, Saprin AN, Vanin AF. [Why does iron abrogate the cytotoxic effect of S-nitrosothiols on human and animal cultured cells?]. Biofizika. 2007; 52: 869-875.

43. Kim YM, Chung HT, Simmons RL, Billiar TR. Cellular non-heme iron content is a determinant of nitric oxide-mediated apoptosis, necrosis, and caspase inhibition. J Biol Chem. 2000; 275: 10954-10961.

44. Lobysheva II, Stupakova MV, Mikoyan VD, Vasilieva SV, Vanin AF. Induction of the SOS DNA repair response in Escherichia coli by nitric oxide donating agents: dinitrosyl iron complexes with thiol-containing ligands and S-nitrosothiols. FEBS Lett. 1999; 454: 177-180.

45. Stupakova MV, Lobysheva II, Mikoyan VD, Vanin AF, Vasilieva SV. A role of iron ions in the SOS DNA repair response induced by nitric oxide in Escherichia coli. Biochemistry (Mosc). 2000; 65: 690-695.

46. Vasil'eva SV, Stupakova MV, Lobysheva II, Mikoyan VD, Vanin AF. Activation of the Escherichia coli SoxRS-regulon by nitric oxide and its physiological donors. Biochemistry (Mosc). 2001; 66: 984-988.

47. Demple B. Signal transduction by nitric oxide in cellular stress responses. Mol Cell Biochem. 2002; 234-235: 11-8.

48. Vasilyeva SV, Strel`tsova DA, Moshkovskaya EY, Vanin AF, Mikoyan VD, Sanina NA, et al. Reversible NO-catalyzed destruction of the Fe-S cluster of the FNR[4Fe-4S]2+ transcription factor: a way to regulate the aidB gene activity in Escherichia coli cells cultured under anaerobic conditions. Doklady Biokhimii i Biofizika. 2010; 435: 283-286.

49. Graziano M, Lamattina L. Nitric oxide and iron in plants: an emerging and converging story. Trends Plant Sci. 2005; 10: 4-8.

50. Gosteev AY, Zorin AV, Rodnenkov OV, Dragnev AG, Chazov EI. Hemodinamic effects of a synthetic analogue of endogenous nitric oxide (II) donors a dinitrosyl iron complexes in hypertensive patients with uncomplicated hypertensive crisis. Therap. Arkhives (Rus). 2014; 9: 49-55.

51. Giliano NY, Konevega LV, Noskin LA, Serezhenkov VA, Poltorakov AP, Vanin AF. Dinitrosyl iron complexes with thiol-containing ligands and apoptosis: studies with HeLa cell cultures. Nitric Oxide. 2011; 24: 151-159.

52. Vernon MW, Wilson EA. Studies on the surgical induction of endometriosis in the rat. Fertil Steril. 1985; 44: 684-694.

53. Bilotas MA, Olivares CN, Ricci AG, Baston JI, Bengochea TS, Meresman GF, et al. Interplay between Endometriosis and Pregnancy in a Mouse Model. PLoS One. 2015; 10: e0124900.

54. Suresh PS, Venkatesh TH, Rajan T, Tsusumi R. Molecular pathology and therapy of endometriosis: revisited. Andrology & Gynecology: Current Research 2013; 1: 3-9.

55. Yochim JM, Blahna DG. Effects of oestrone and progesterone on collagen and ascorbic acid content in the endometrium and myometrium of the rat. J Reprod Fertil. 1976; 47: 79-82.

56. Fontecave M. Ribonucleotide reductases and radical reactions. Cell Mol Life Sci. 1998; 54: 684-695.

57. Mier-Carbrera J, Gonzalez-Gallardo S, Hernandez-Guerrero C. Effect of nitric oxide and Th1/Th2 cytokine supplementation over ectopic endometrial tissue growth in a murine model of endometriosis. Reproductive Science 2013; 20: 1332–1338.

58. Vanin AF, Huisman A, van Faassen EE. Iron dithiocarbamate as spin trap for nitric oxide detection: pitfalls and successes. Methods Enzymol. 2002; 359: 27-42.

59. Toledo JC, Bosworth CA, Hennon SW, Mahtani HA, Bergonia HA, Lancaster JR. Nitric oxide-induced conversion of cellular chelatable iron into macromolecule-bound paramagnetic dinitrosyliron complexes. J Biol Chem. 2008; 283: 28926-28933.

60. Adamyan LV, Kulakov VI. Endometriosis: guidance for physicians. Moscow: Medicine PH. 1998.

61. Alagiri M, Chottiner S, Ratner V, Slade D, Hanno PM. Interstitial cystitis: unexplained associations with other chronic disease and pain syndromes. Urology. 1997; 49: 52-57.

62. Sinaii N, Cleary SD, Ballweg ML, Nieman LK, Stratton P. High rates of autoimmune and endocrine disorders, fibromyalgia, chronic fatigue syndrome and atopic diseases among women with endometriosis: a survey analysis. Hum Reprod. 2002; 17: 2715-2724.

63. Giamberardino MA, De Laurentis S, Affaitati G, Lerza R, Lapenna D, Vecchiet L. Modulation of pain and hyperalgesia from the urinary tract by algogenic conditions of the reproductive organs in women. Neurosci Lett. 2001; 304: 61-64.

64. Demir F, Ozcimen EE, Oral HB. The role of gynecological, urological, and psychiatric factors in chronic pelvic pain. Arch Gynecol Obstet. 2012; 286: 1215-1220.

65. Berkley KJ, Rapkin AJ, Papka RE. The pains of endometriosis. Science. 2005; 308: 1587-1589.

66. Stratton P, Berkley KJ. Chronic pelvic pain and endometriosis: translational evidence of the relationship and implications. Hum Reprod Update. 2011; 17: 327-346.

67. McAllister SL, Dmitrieva N, Berkley KJ. Sprouted innervation into uterine transplants contributes to the development of hyperalgesia in a rat model of endometriosis. PLoS One. 2012; 7: e31758.

68. Zhang G, Dmitrieva N, Liu Y, McGinty KA, Berkley KJ. Endometriosis as a neurovascular condition: estrous variations in innervation, vascularization, and growth factor content of ectopic endometrial cysts in the rat. Am J Physiol Regulatory Integrative Comp Physiol. 2008; 294: 162 - 171.

69. Cury Y, Picolo G, Gutierrez VP, Ferreira SH. Pain and analgesia: The dual effect of nitric oxide in the nociceptive system. Nitric Oxide. 2011; 25: 243-254.

70. Schmidtko A, Tegeder I, Geisslinger G. No NO, no pain? The role of nitric oxide and cGMP in spinal pain processing. Trends Neurosci. 2009; 32: 339-346.

71. Schmidtko A, Gao W, Sausbier M, Rauhmeier I, Sausbier U, Niederberger E, et al. Cysteine-rich protein 2, a novel downstream effector of cGMP/cGMP-dependent protein kinase I-mediated persistent inflammatory pain. J Neurosci. 2008; 28: 1320-1330.

72. Tegeder I, Scheving R, Wittig I, Geisslinger G. SNO-ing at the nociceptive synapse? Pharmacol Rev. 2011; 63: 366-389.

73. Arnold C, Lamp J, Lamp O, Einspanier A. Behavioral tests as indicator for pain and distress in a primate endometriosis model. J Med Primatol. 2011; 40: 317-326.

74. Adamyan LV, Burgova EN, Tkachev NA, Mikoyan VD, Stepanyan AA, Tsyganov AA, et al. Dinitrosyl iron complexes with glutathione reduce the pain in rats with experimental endometriosis. Problemy Reproduktsii (Rus). 2013; 5:73-80.

75. Vanin AF, Ostrovskaia LA, Korman DB, Mikoyan VD, Kubrina LN, Borodulin MM, et al. [Anti-nitrosative system as a factor of malignant tumor resistance to cytotoxic effect of nitrogen monooxide]. Biofizika. 2015; 60: 152-157.

76. Green J, Rolfe MD, Smith LJ. Transcriptional regulation of bacterial virulence gene expression by molecular oxygen and nitric oxide. Virulence. 2013; 5: 1-33.

77. Lakomkin VL, Vanin AF, Timoshin AA, Kapelko VI, Chazov EI. Long-lasting hypotensive action of stable preparations of dinitrosyl-iron complexes with thiol-containing ligands in conscious normotensive and hypertensive rats. Nitric Oxide. 2007; 16: 413-418.

Austin J Reprod Med Infertil - Volume 2 Issue 4 - 2015
ISSN : 2471-0393 | www.austinpublishinggroup.com

Citation: Vanin AF, Burgova EN and Adamyan LV. Dinitrosyl Iron Complexes with Glutathione Suppress Surgically Induced Experimental Endometriosis in Rats. Austin J Reprod Med Infertil. 2015; 2(4): 1019.